A robust method for fabrication of monodisperse magnetic mesoporous silica nanoparticles with core-shell structure as anticancer drug carriers

Asgari, Mahsa; Soleymani, Meysam; Miri, Taghi; Barati, Abolfazl

DOI:
10.1016/j.molliq.2019.111367

Document Version
Peer reviewed version

Citation for published version (Harvard):
Asgari, M, Soleymani, M, Miri, T & Barati, A 2019, 'A robust method for fabrication of monodisperse magnetic mesoporous silica nanoparticles with core-shell structure as anticancer drug carriers', *Journal of Molecular Liquids*, vol. 292, 111367. https://doi.org/10.1016/j.molliq.2019.111367

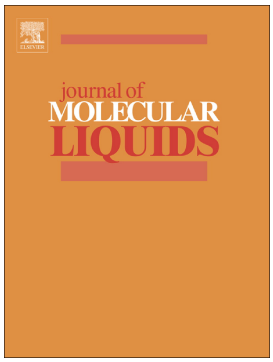

A robust method for fabrication of monodisperse magnetic mesoporous silica nanoparticles with core-shell structure as anticancer drug carriers

Mahsa Asgari, Meysam Soleymani, Taghi Miri, Abolfazl Barati

PII: S0167-7322(19)32990-3
DOI: https://doi.org/10.1016/j.molliq.2019.111367
Article Number: 111367
Reference: MOLLIQ 111367

To appear in: *Journal of Molecular Liquids*

Received date: 27 May 2019
Revised date: 9 July 2019
Accepted date: 12 July 2019

Please cite this article as: M. Asgari, M. Soleymani, T. Miri, et al., A robust method for fabrication of monodisperse magnetic mesoporous silica nanoparticles with core-shell structure as anticancer drug carriers, Journal of Molecular Liquids, https://doi.org/10.1016/j.molliq.2019.111367

A Robust Method for Fabrication of Monodisperse Magnetic Mesoporous Silica Nanoparticles with Core-shell structure as Anticancer Drug Carriers

Mahsa Asgari[1], Meysam Soleymani[1,*], Taghi Miri[1,2], Abolfazl Barati[1]

[1] Department of Chemical Engineering, Faculty of Engineering, Arak University, Arak,38156-88349, Iran

[2] School of Chemical Engineering, University of Birmingham, B15 2TT, UK

Email of Corresponding Author: m-soleymani-chem@araku.ac.ir

Abstract

This paper presents a novel method based on an inverse microemulsion system to synthesize monodisperse magnetic mesoporous silica nanoparticles (MMSN) with core-shell structure. In this method, the water-in-oil microemulsion system was prepared using of cyclohexane containing silica precursor as a continuous oil phase, discrete water droplets containing magnetic seeds (Fe_3O_4 nanoparticles) and urea as an aqueous phase, and cetyltrimethylammonium bromide (CTAB) and 1-butanol as a surfactant and co-surfactant, respectively. Unlike the traditional reverse microemulsion method, the magnetic seeds used in this system were first covered by a self-organized two-layer surfactant including oleic acid and CTAB as a good host for silica formation. Hence, by removing the CTAB template from the silica structure, a mesoporous silica shell remains on the surface of Fe_3O_4 nanoparticles. The effects of catalyst types (urea and NaOH), TEOS content, and reaction temperature on the morphology and size of the prepared samples were investigated. It was found that by rising the reaction temperature from 70 to 120°C, the thickness of the silica layer was increased from 3 to 17 nm. Moreover, a thicker silica coating (26 nm) was obtained by increasing the TEOS content. Also, the performance of the prepared nanocomposite for drug delivery applications was investigated using 5-fluorouracil (5-Fu) as a drug model in a physiological medium. The obtained results showed that the prepared magnetic mesoporous silica nanocomposite has great potential for biomedical applications.

Keywords: Core-shell structure, Fe_3O_4 nanoparticles, Mesoporous silica, Inverse microemulsion, Drug delivery

1. Introduction

Over the last two decades, many efforts have been devoted to the fabrication of novel drug delivery systems which can release drug molecules at the specific tissue in a controlled manner [1-3]. To date, many kinds of organic and inorganic materials have been investigated as drug carriers including hydrogels [4, 5], liposomes [6, 7], silica nanoparticles [8], dendrimers [9], etc. Among these materials, mesoporous silica nanoparticles (MSN) received a great deal of attention because of their significant advantages such as high surface area, large pore volume, low apparent cytotoxicity, easy surface modification, and good stability in the most chemical and biological environments [10-12]. The combination of silica with magnetic nanoparticles (such as Fe_3O_4, $La_{1-x}Sr_xMnO_3$, and $CoFe_2O_4$, etc.), in a core-shell structure led to an ideal system for different biological applications such as magnetic hyperthermia therapy [13], magnetic resonance imaging [14], and drug delivery systems [15]. Many works have studied the influence of morphology and porosity of the core-shell MMSNs on the performance of nanocomposites as drug carriers [16-18]. It has been found that, the nanoparticles (less than 100 nm) can easily pass the biological barriers, and subsequently, improve the passive targeting through the EPR effect [19]. However, the nanoparticles larger than 100 nm were rapidly removed from the blood circulation by the reticuloendothelial system [20]. Besides, some researchers have investigated the influence of the size of silica nanoparticles on the level of cell cytotoxicity [21, 22]. These studies proved that the smaller sized silica particles had caused higher toxicity in the tumor cells. Although much work has been done on the synthesis of MMSN, the achievement of monodispersed nanoparticles with a suitably small size is still challenging.

Generally, there have been reported two main approaches for the fabrication of magnetic silica nanoparticles with core-shell structure, namely, stober method and reverse microemulsion technique [23]. Although the stober method has been commonly used to fabricate the magnetic mesoporous silica, only a few works have successfully reported the synthesis of monodisperse core-shell nanocomposites with a controlled shell thickness [19, 24, 25]. In this process, due to the direct addition of silica precursor to the aqueous reaction medium, the hydrolysis and growth of silica on the surface of nanoparticles occur very fast and in an uncontrollable way [26]. Moreover, many other parameters such as reaction temperature, stirring speed, and the ratio of the reactants can strongly influence the size and morphology of the product [27]. As a result, the stober method is rather complicated and unrepeatable to fabricate the core-shell nanocomposite

with the appropriate size for specific biomedical applications. On the other hand, the reverse microemulsion method is an alternative approach to synthesize the core-shell Fe_3O_4@SiO_2 nanoparticles [23]. In this method, the hydrolysis and condensation reactions occur only within the discrete water droplets which were well dispersed in an organic phase stabilized by one or two surfactants. Therefore, this method could prevent the aggregation phenomenon during the silica growth on the surface of magnetic nanoparticles. For example, Toprak and co-workers successfully fabricated monodispersed core-shell nanocomposites with the size smaller than 100 nm via controlling the reaction time and precursor concentration in an inverse microemulsion system using Triton-X100/hexanol/water/cyclohexane [28]. However, the inverse microemulsion method produces a nonporous silica layer on the surface of nanoparticles. Hence, it would be rather difficult to obtain a good drug storage with sustained and controllable drug release using this method, and as a result, the application of the prepared carrier for drug delivery will be limited [29].

To solve these problems, a novel strategy is presented in the current research for the fabrication of magnetic nanoparticles with a mesoporous silica shell based on the modified inverse microemulsion method. In the proposed method, the oleic acid-coated Fe_3O_4 nanoparticles were first synthesized by the thermal decomposition of iron acetylacetonate in dibenzylether. Then, the hydrophobic nanoparticles were transferred to the aqueous phase using CTAB as an outer layer surfactant as well as a soft removable template. The prepared water-dispersible nanoparticles were then used as nucleation seeds for silica formation in the aqueous phase of a microemulsion system containing CTAB/1-butanol/cyclohexane/water. Finally, the mesoporous silica shell was formed on the surface of magnetic nanoparticles by removing CTAB template from the structure using a calcination process. Moreover, the thickness of the silica coating was controlled by changing the silica precursor content and also the temperature of the reaction. Also, the efficacy of the prepared sample for drug delivery application was investigated using 5-Fu as a drug model which is commonly used to treat different diseases such as breast and stomach cancers.

2. Experimental Section

Iron (III) acetylacetonate (99%), dibenzylether (98%), cyclohexane (99%), hexadecyltrimethylammonium bromide (CTAB, 97%), oleylamine (technical grade, 70%),

tetraethyl orthosilicate (TEOS, 98%) were purchased from Merck company, Germany. Urea (99%), 1-butanol (99%), 5-fluorouracil (5-Fu), ethanol and chloroform were obtained from Sigma Aldrich, Germany. Oleic acid was purchased from Daejung Chemicals, Korea. All materials and solvents was used as received and without any purifications.

2.2 Synthesis of Fe_3O_4 nanoparticles

Fe_3O_4 nanoparticles were synthesized by a slightly modified thermal decomposition method [30]. In a typical synthesis, 1.41 g of $Fe(acac)_3$ was added to a mixture of dibenzylether (30 mL), oleic acid (0.6 mL) and oleylamine (1.31 mL). Then, the temperature of the suspension was raised to 120 °C and held at this temperature for 30 min under nitrogen atmosphere. Then, the mixture was quickly heated to 280 °C and kept at this temperature for 4 h. After cooling the suspension to the room temperature, the solution was centrifuged at 10000 rpm for 15 min and washed by ethanol three times. Finally, the oleic acid-stabilized Fe_3O_4 nanoparticles were dispersed in chloroform for further use.

2.3 Phase transfer of oleic acid-capped Fe_3O_4 nanoparticles

One mL of the as-prepared Fe_3O_4 nanoparticles dispersed-in-chloroform was mixed with an aqueous solution containing 0.06 g CTAB [26]. The obtained macroemulsion was sonicated for 1 h (Ultrasonic Bath, Eurosonic 4 D, Euronda, Italy) and then heated to 70 °C for 10 min to evaporate chloroform leading to a stable transparent solution containing water dispersible Fe_3O_4 nanoparticles. To remove the excess surfactant from the nanoparticle suspension, the solution was cooled down to 5 °C and then centrifuged to separate the excess amount of surfactant.

2.4 Synthesis of magnetic mesoporous silica nanocomposite (Fe_3O_4@$mSiO_2$)

Magnetic mesoporous silica nanocomposites were fabricated using a modified inverse microemulsion method using CTAB/1-butanol/water/cyclohexane as surfactant/co-surfactant/aqueous phase/organic phase [31]. In a typical synthesis, 2 g of CTAB was added to a mixture of 1-butanol and cyclohexane at room temperature. Subsequently, by addition of 3 mL of an aqueous suspension containing CTAB-stabilized Fe_3O_4 nanoparticles and urea to the above solution, a transparent microemulsion system was formed. Then, a certain amount of TEOS was added to the prepared microemulsion under vigorous stirring. The obtained microemulsion was

then transferred to a 75 mL Teflon-lined autoclave and heated at the desired temperature for 12 h. The formed core-shell $Fe_3O_4@SiO_2$ nanoparticles were collected by centrifugation (4000 rpm) (Premium Centrifuge, Pole Ideal Tajhiz Co., Iran) and then washed with ethanol and water three times and then dried in an oven at 60 °C. Finally, for the extraction of CTAB from the silica shell, a calcination process was utilized based on heating the nanocomposites at 550°C for 6 h [32].

2.5 In vitro biocompatibility

The colorimetric methyl thiazolyl tetrazolium (MTT) assay was carried out to investigate the biocompatibility of the $Fe_3O_4@mSiO_2$ nanoparticles. To this end, MCF-7 cells were seeded into a 96-well plate and cultured in DMEM medium neutralized with 10% FBS and incubated for 24 h at 37 °C in a humidified 5% CO_2 atmosphere. Then, the cells were further incubated with the $Fe_3O_4@mSiO_2$ nanoparticles with different concentrations (0, 10, 25, 50, 100, and 200 μg mL^{-1}) for 24 h. Afterward, MTT reagent was added to each well and was incubated for another 4 h. The cell viability was measured by evaluating the optical density at 570 nm.

2.6 Drug loading and releasing procedure

For drug loading, 0.4 ml of 5-Fu (50 mg mL^{-1}) was dissolved in 20 ml DMSO. Afterward, 0.02 g of as-synthesized MMSN was added to the above solution [33]. The dispersion was magnetically stirred for 48 h at room temperature. The drug-loaded nanoparticles were separated by centrifugation, and then, the amount of 5-Fu in the supernatant was determined using UV spectrophotometry at a wavelength of 266 nm. The drug loading content was calculated according to equation 1 [34]:

$$\text{Drug loading (\%)} = \frac{\text{Initial weight of drug} - \text{Weight of drug in supernatant solution}}{\text{Weight of drug loaded nanocomposite}} \times 100 \quad (1)$$

To obtain the drug release profile of 5-Fu from MMSN, the drug-loaded MMSN were immersed in 100 ml of PBS solution. It should be noted that the solution was kept under the stirring condition at 37 °C. At the specific time intervals, one ml of the release medium was withdrawn, and after centrifugation, the amount of the drug released was determined using UV-vis

spectrophotometer at 266 nm. After each sampling, one ml of PBS solution was added to the release medium to keep the total volume of solution constant.

2.7 Characterization

Fourier Transform Infrared Spectroscopy (FTIR) analysis was performed using an ALPHA II FTIR Spectrometer, BrukerOptik GmbH. Vibrating sample magnetization (VSM) analysis was measured at room temperature using Lake Shore Cryotronics, Model 7407. X-ray diffraction (XRD) patterns were obtained using a Panalytical X'PertPro diffractometer (Holland) with CuKα radiation (λ=1.54 angstrom). The morphology of the prepared nanoparticles was studied using transmission electron microscopy (TEM, Philips-CM120). UV–vis absorption spectra were recorded on a UV-1050 spectrophotometer (PerkinElmer).

3. Results and discussions

In this work, the thermal decomposition method was used to synthesize the oleic acid-capped Fe_3O_4 nanoparticles. The fabricated oleic acid-capped Fe_3O_4 nanoparticles were dispersible in organic media such as chloroform and hexane. To make the water-dispersible nanoparticles, the phase transfer of hydrophobic nanoparticles from the organic phase to the aqueous medium was performed using CTAB surfactant. In fact, in this process, Van der Waals interactions between the alkyl chains of CTAB and oleic acid may result in the self-assembly of CTAB as an outer layer on the surface of nanoparticles. The obtained hydrophilic nanoparticles were then used as nucleation seeds in the inverse microemulsion system to synthesize the magnetic mesoporous silica.

To this end, the inverse microemulsion system was first formed using CTAB as the main surfactant, 1-butanol as a co-surfactant, cyclohexane containing silica precursor as a continuous oil phase, and discrete water droplets containing urea and nucleation seeds as the aqueous phase. A proposed mechanism for the formation of core-shell nanocomposites is schematically depicted in Fig. 1. After the addition of silica precursor (TEOS) to the oil phase, the molecules of TEOS hydrolyzed at the interface of water droplets and then condensed on the surface of the CTAB-Fe_3O_4 nanoparticles. In this condition, the organic phase could slow down the rate of diffusion of TEOS to the aqueous phase. As a result, the TEOS hydrolysis would become more controllable, leading to the monodisperse nanoparticles without any aggregations. Finally, by extracting the

CTAB molecules from the structure via the calcination process, the silica shell with high porosity could be obtained.

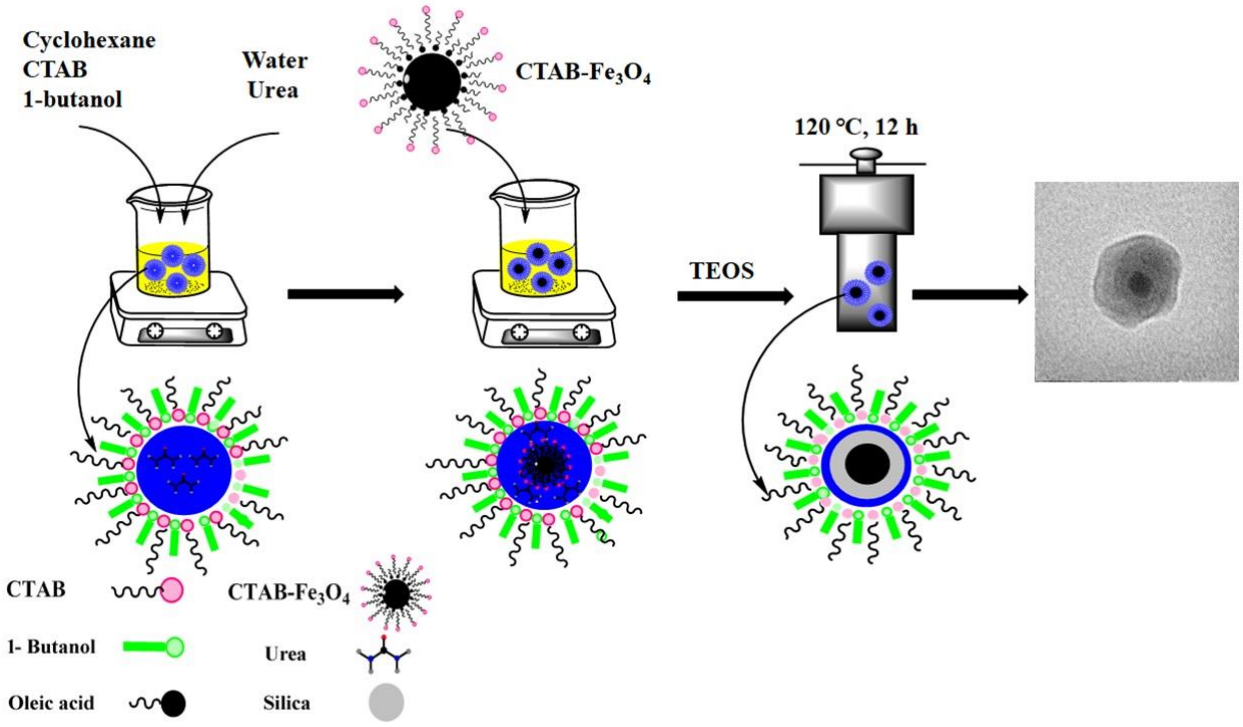

Fig. 1: Schematic representation of Fe_3O_4@$mSiO_2$ nanoparticles by modified inverse microemulsion method

FTIR analysis was carried out to investigate the surface functional groups and the integrity of nanoparticles formation. Fig. 2 shows the FTIR spectra for the oleic acid-coated Fe_3O_4 nanoparticles dispersed in chloroform, CTAB-Fe_3O_4 and Fe_3O_4@$mSiO_2$ nanoparticles in powder form. In the oleic acid-coated Fe_3O_4 spectrum, the absorption peak at 680 cm^{-1} is associated with the stretching mode of the Fe–O bond in the magnetite nanoparticles. The sharp peak appeared at the 772 cm^{-1} is attributed to the chloroform. The two absorption peaks at 2925 cm^{-1} and 2854 cm^{-1} are assigned to the asymmetric and symmetric stretch vibration modes of the $-CH_2$ groups, and the weak band at 1741 cm^{-1} can be ascribed to the stretching mode of the abandoned C=O bond in the oleic acid [30]. The peak at 1440 cm^{-1} is also assigned to the stretch vibration of $-COO^-$ groups [35]. Together these results confirm that the oleic acid was coated on the surface of the

Fe_3O_4 NPs. Also, the FTIR spectrum of the oleic acid-coated Fe_3O_4 nanoparticles after phase transfer to the aqueous phase using CTAB is shown in Fig. 2b. The absorption bands at 2849 cm^{-1} and 1450 cm^{-1} are attributed to the stretching vibrations of C-H and C-N bonds of CTAB, respectively [36]. The appearance of as-described peaks proves the interactions between oleic acid and CTAB molecules.

Fig. 2c shows the FTIR spectrum for the Fe_3O_4@mSiO_2 nanoparticles. The two characteristic absorption peaks appeared at 1104, and 802 cm^{-1} are related to the Si-O-Si stretching and Si-O bending modes, respectively, which further proves that SiO_2 shell has been successfully covered the surface of Fe_3O_4 nanoparticles [37]. It is worthy to note that the characteristic peak for the Fe_3O_4 nanoparticles appeared at 638 cm^{-1} with a lower intensity which could confirm the surface coating of the magnetite nanoparticles with a silica shell. Also, the peak intensity of the C–H band (2849 cm^{-1} and 2918 cm^{-1}) from CTAB surfactants is much lower than that for the Fe_3O_4@mSiO_2 which is due to the extraction of CTAB from the silica shell.

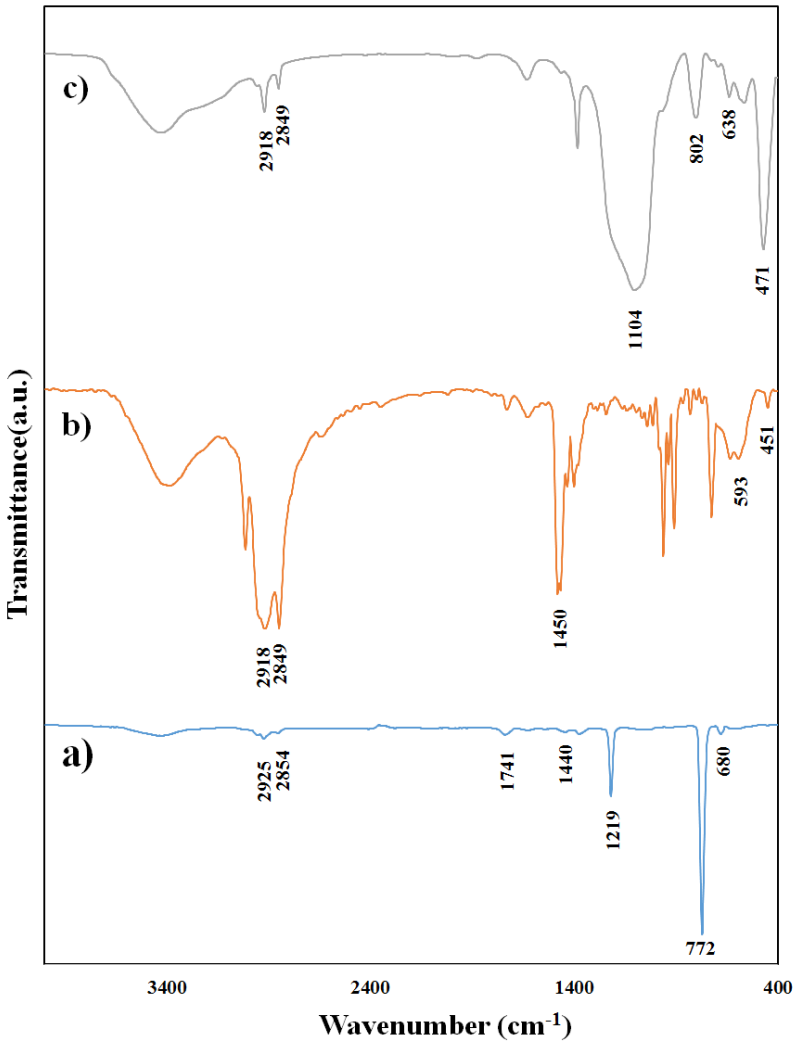

Fig. 2: FTIR patterns of a) oleic acid-Fe_3O_4, b) CTAB-Fe_3O_4, and c) Fe_3O_4@$mSiO_2$

Fig. 3 shows the XRD spectra for the as-synthesized Fe_3O_4 and Fe_3O_4@$mSiO_2$ nanoparticles. All diffraction peaks in the XRD pattern of the as-prepared Fe_3O_4 nanoparticles (Fig. 3a) are in good agreement with the standard Fe_3O_4 diffraction pattern (Card No. 75-0033) confirming the successful fabrication of the Fe_3O_4 nanoparticles. Also, the broad characteristic peak appeared at around 20° in the XRD pattern of the Fe_3O_4@$mSiO_2$ (Fig. 3b) could be related to the amorphous silica which indicates the formation of silica layer on the surface of magnetite nanoparticles.

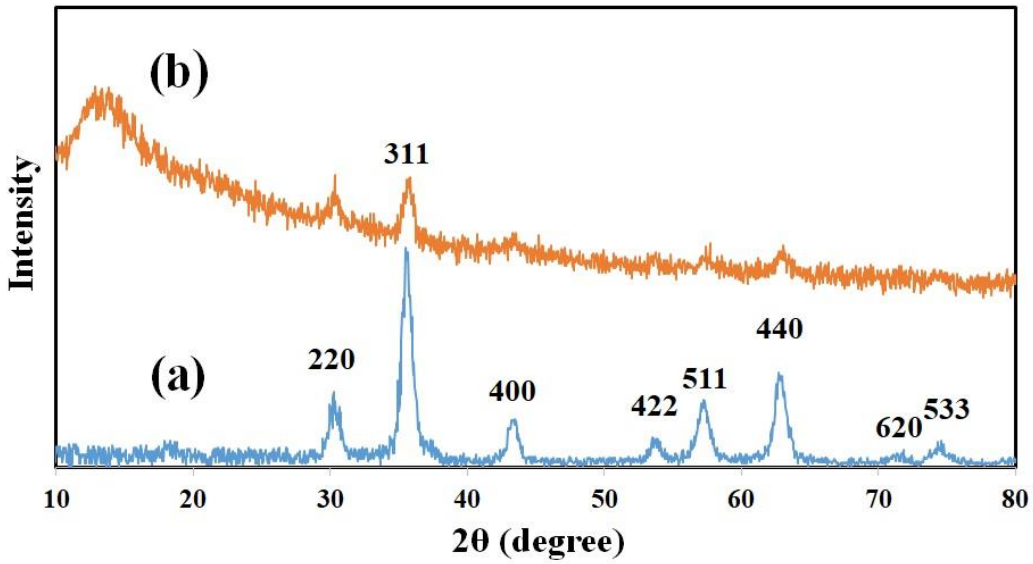

Fig. 3: XRD spectra of a) oleic acid-Fe_3O_4, and b) Fe_3O_4@mSiO_2

The TEM image of the as-prepared Fe_3O_4 nanoparticles and the corresponding particle size distribution is shown in Fig. 4. As can be seen, the obtained nanoparticles are uniform in size with a nearly spherical shape and the average particle size distribution of the product, calculated based on the Ferret-diameter for more than 250 particles, is about 16.4 nm.

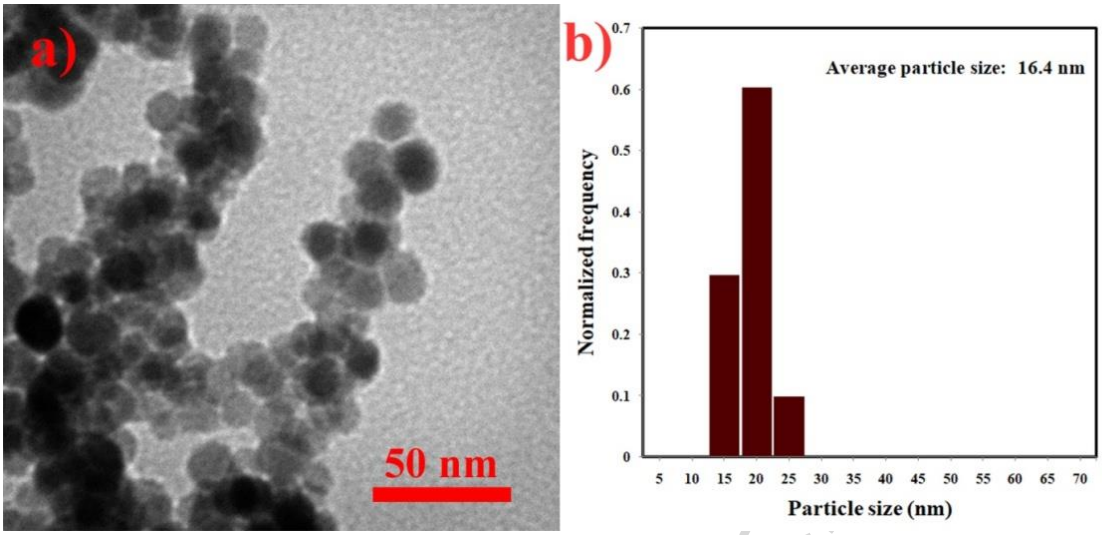

Fig. 4: TEM image of a) Fe_3O_4 nanoparticles, and b) particle size distribution

To obtain the core-shell nanocomposite with controllable size and morphology, the roles of different experimental parameters were investigated. At first, the effect of the catalyst type (NaOH and urea) on the morphology and monodispersity of the synthesized nanoparticles was studied. To this end, 0.1 M NaOH solution was first used to supply OH^- ions within the synthesis medium. In this condition, before to the addition of 0.06 mL TEOS, the pH value of the aqueous phase in microemulsion system was adjusted to 10 using NaOH solution, and the reaction process was carried out at 70°C for 12 h. In the case of urea, a certain amount of urea was fed to the aqueous phase according to the experimental procedure. Figs. 5a and 5b show the TEM images of prepared nanoparticles using NaOH, and Urea as basic catalysts, respectively. It seems that upon using NaOH as a basic catalyst, the magnetite nanoparticles would be trapped within the connected silica clusters and an aggregated composite was obtained. It could be explained that by using NaOH as a catalyst, the growth of silica was fast and uncontrollable. On the other hand, when urea was used in the reaction, a uniform coating of silica was formed on the surface of Fe_3O_4 nanoparticles, and thus, composite with core-shell structure was achieved. In fact, when urea was used as a catalyst, the OH^- ions were slowly produced in the reaction medium by hydrolysis of urea[38]. Therefore, the hydrolysis rate of TEOS can be regulated using urea as a weak basic catalyst, which results in the formation of a nanocomposite with core-shell structure.

Also, the effect of reaction temperature (70 and 120 °C) on the size of nanocomposites was studied while the amount of TEOS was kept at 0.06 ml for both samples. As can be seen in Fig.

5c, a thin layer of silica with a thickness of about 3 nm was obtained at a temperature of 70 °C. By increasing the reaction temperature up to 120°C, the thickness of the silica layer reached to about 17 nm (see Fig. 5d). This phenomenon could be due to the increasing of the hydrolysis and condensation rate of TEOS upon rising the reaction temperature. Furthermore, to synthesize core-shell nanoparticles with different shell thicknesses, different amounts of TEOS (0.06 and 1.2 mL) were added to the microemulsion and the reaction process was carried out at 120 °C for 12 h. As shown in Figs. 5d and 5e, by increasing the amount of TEOS from 0.06 to 1.2 mL, the thickness of the silica layer was increased from 17 to about 26 nm.

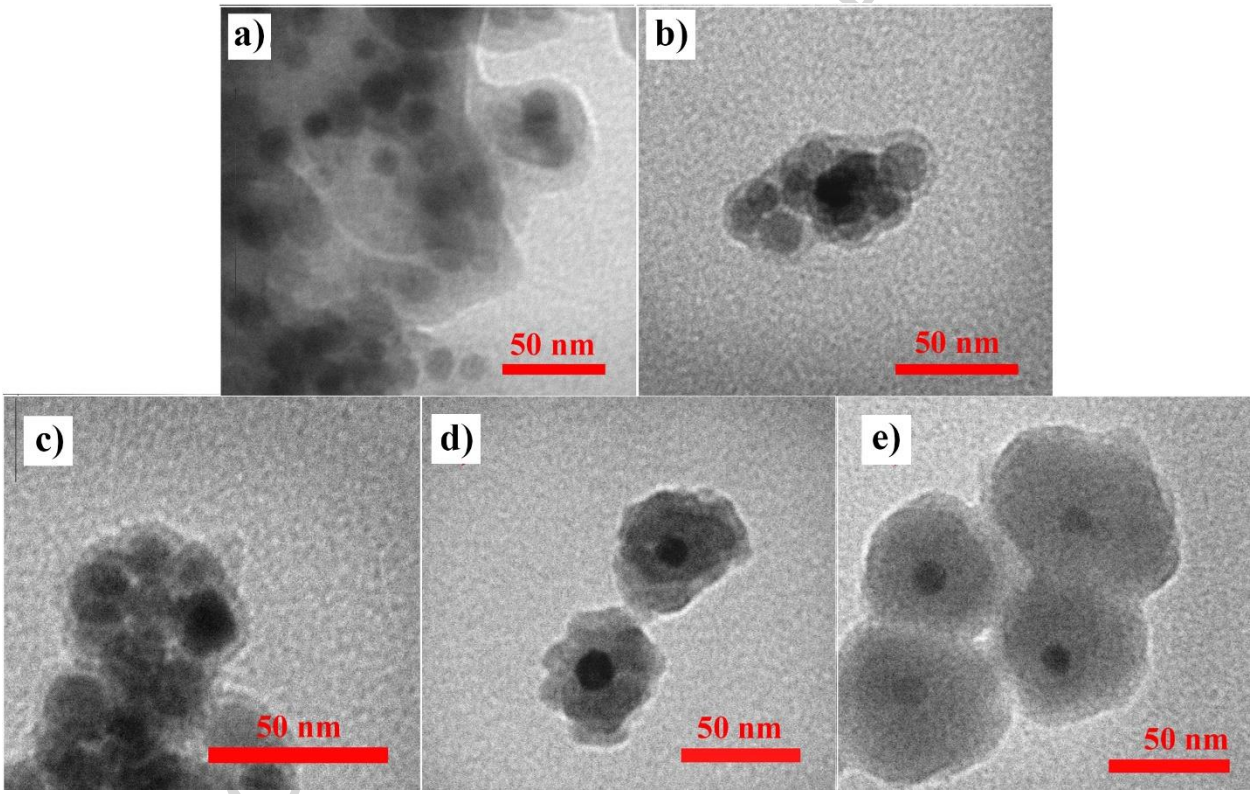

Fig. 5: TEM image of Fe_3O_4@$mSiO_2$ nanoparticles, (a) with NaOH, (b) with Urea. Fe_3O_4@$mSiO_2$ with shell thicknesses of (c) 3nm, (d) 17 nm and (e) 26nm.

The porosity of the synthesized magnetic mesoporous silica was evaluated by N_2 adsorption–desorption isotherms. Fig. 6 shows the N_2 adsorption/desorption curve of the MMSN, which can be classified as Type IV isotherms. In this curve, a hysteresis loop, formed by capillary condensation of N_2, indicates a mesoporous structure for the silica shell. The surface area

(calculated based on BET method), total pore volume, and mean pore diameter of the MMSN with silica thickness of about 26 nm were 153.74 $m^2 g^{-1}$, 0.679 $cm^3 g^{-1}$, and 3.6 nm, respectively.

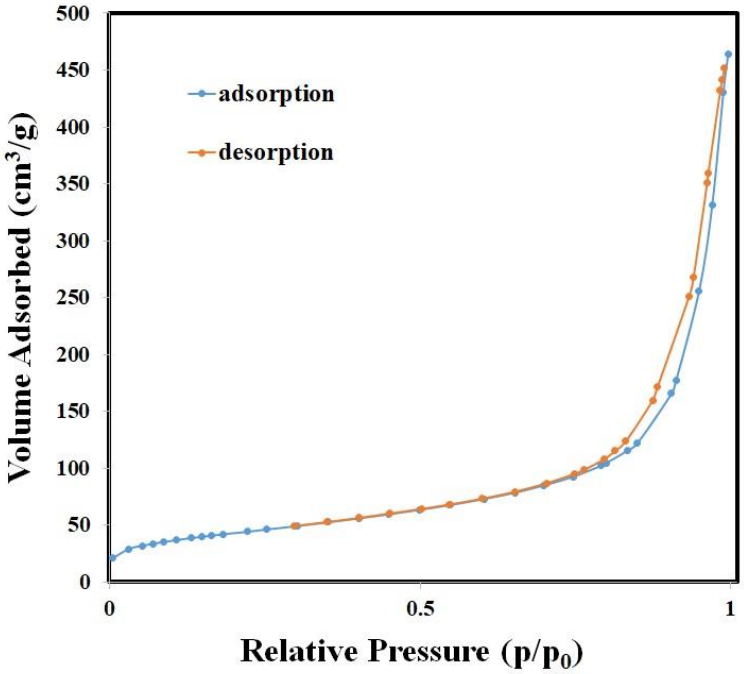

Fig. 6: Nitrogen adsorption-desorption isotherms of the Fe_3O_4@$mSiO_2$

The magnetic properties of the as-synthesized Fe_3O_4 nanoparticles and magnetic mesoporous silica nanocomposite were investigated using VSM analysis. According to the magnetization curves presented in Fig. 7, one could infer that both samples conform to the superparamagnetic regime because no hysteresis loop was detected in the magnetization curves. The saturation magnetization (Ms) of the as-synthesized Fe_3O_4 and Fe_3O_4@$mSiO_2$ nanoparticles reached to 63.83 and 4.8 emu g^{-1}, respectively. The sharp decline in Ms for Fe_3O_4@$mSiO_2$ nanoparticles may be attributed to the presence of diamagnetic silica layer on the surface of Fe_3O_4 nanoparticles [24, 26, 39]. However, the prepared nanocomposite exhibited a relatively good response to the magnetic field which promises great potential for the prepared product to be used as targeted drug delivery systems.

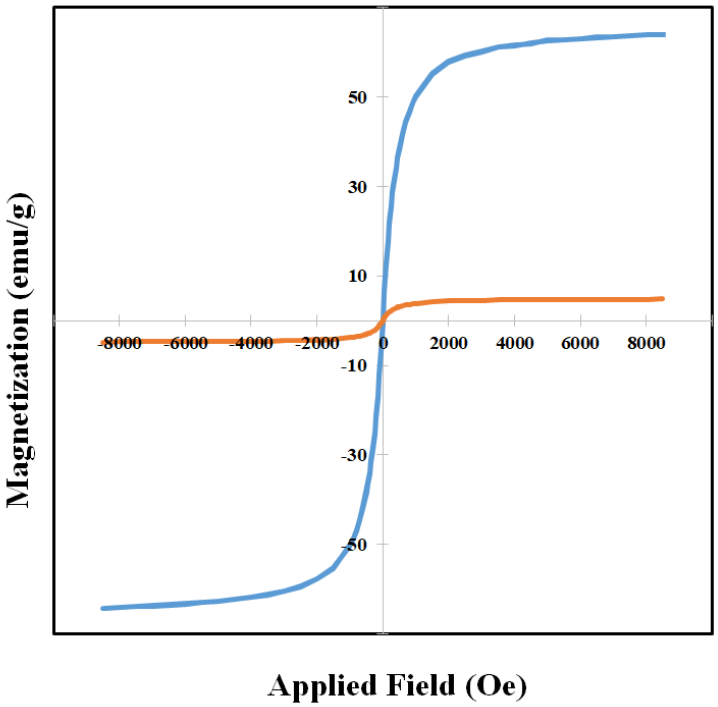

Fig. 7: Magnetization curve of a) Fe_3O_4 nanoparticles capped with oleic acid, and b) Fe_3O_4@mSiO_2

3.8 In vitro Biocompatibility

The MTT assay was carried out to evaluate the biocompatibility of the mesoporous silica-coated Fe_3O_4 nanoparticles. Fig. 8a shows the cell viability of MCF-7 cells after 24 h exposure to the nanoparticles at different concentrations. After the incubation period, the viability of MCF-7 cells were more than 90% at all concentrations of the nanoparticles. These results suggested that the MMSN possess rather good biocompatibility which is considered as one of the major requirements for drug delivery applications.

3.9 Drug Loading and Release

5-fluorouracil (5-Fu) is widely used as an anticancer drug for the treatment of a variety of cancers such as colon, skin, and breast cancer. In this study, the synthesized MMSN with 26 nm silica layer was chosen for drug delivery experiments. First, the drug loading experiments were carried out by soaking the sample in the solution of 5-Fu in DMSO. The drug loading content, calculated based on UV–vis measurements, was about 49±5 mg/g_{MMSN}. This result is in accordance with the drug loading content reported for the magnetic mesoporous silica nanocomposites [33, 40]. The absorption curves obtained at different concentrations are shown

in the inset of Fig. 8b. The drug release profile of 5-Fu from the MMSN is depicted in Fig. 8b. The results show that there is an initial burst release in the first 4 h of starting experiment, which could be attributed to the fast desorption of drug molecules adsorbed on the exterior surface of the nanocomposites. Following the initial burst-like release, a sustained release was observed, which could be due to the diffusion of 5-Fu molecules located into the pores of silica layer to the releasing medium. As can be seen, the release curve reaches a plateau after 40 h.

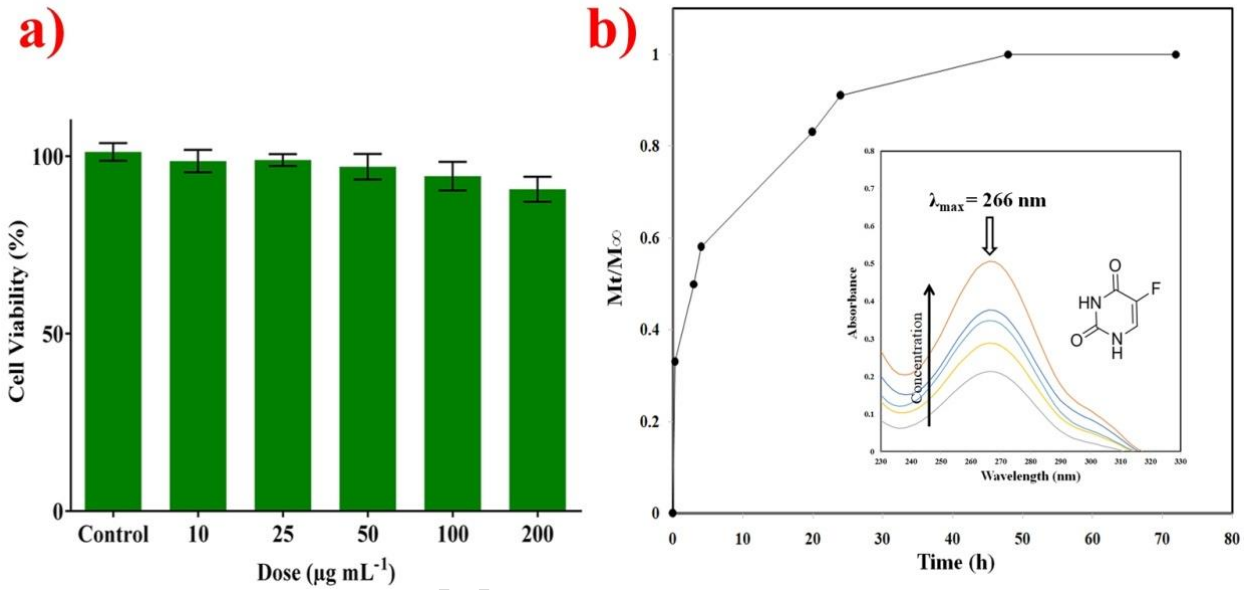

Fig.8: a) In vitro cytotoxicity experiments of MCF-7 cells incubated with different concentration of Fe_3O_4@$mSiO_2$, b) 5-FU release profile from Fe_3O_4@$mSiO_2$ nanoparticles at pH=7.4

3. Conclusions

In summary, we presented a modified inverse microemulsion method to synthesize magnetic mesoporous silica with a core-shell structure. The inverse microemulsion was formed by using CTAB, cyclohexane, 1-butanol, and water. In this study, the thermal decomposition method was used to fabricate Fe_3O_4 nanoparticles functionalized by oleic acid. Water-dispersible products were obtained by phase transferring nanoparticles using CTAB. Then CTAB-Fe_3O_4 nanoparticles were used as seeds for the formation and growth of silica in the microemulsion system. The average size of the prepared core-shell nanocomposite is below 100 nm in diameter. Also, the thickness of the silica shell could be adjusted by changing TEOS content and temperature of the reaction. Furthermore, the behavior of drug release proved that the prepared core-shell

nanocomposite could be used for cancer therapy. Also, the prepared core-shell nanocomposite could be applicable for hyperthermia and MRI applications.

References

1. A.A. Moghanjoughi, D. Khoshnevis, A. Zarrabi, A concise review on smart polymers for controlled drug release, Drug Delivery Transl. Res. 6 (2016) 333-340. https://doi.org/10.1007/s13346-015-0274-7.
2. J.F. Coelho, P.C. Ferreira, P. Alves, R. Cordeiro, A.C. Fonseca, J.R. Góis, M.H. Gil, Drug delivery systems: Advanced technologies potentially applicable in personalized treatments, EPMA journal. 1 (2010) 164-209.https://doi.org/10.1007/s13167-010-0001-x.
3. J. Shi, A.R. Votruba, O.C. Farokhzad, R. Langer, Nanotechnology in drug delivery and tissue engineering: from discovery to applications, Nano Lett. 10 (2010) 3223-3230.https://doi.org/ 10.1021/nl102184c.
4. G. Deen, X. Loh, Stimuli-Responsive Cationic Hydrogels in Drug Delivery Applications, Gels. 4 (2018) 13.https://doi.org/10.3390/gels4010013.
5. E. Larrañeta, S. Stewart, M. Ervine, R. Al-Kasasbeh, R. Donnelly, Hydrogels for hydrophobic drug delivery, Classification, synthesis and applications, J Funct Biomater. 9 (2018) 13. https://doi.org/10.3390/jfb9010013.
6. S.Z. Vahed, R. Salehi, S. Davaran, S. Sharifi, Liposome-based drug co-delivery systems in cancer cells.Mater. Sci. Eng. C. 71 (2017) 1327-1341.https://doi.org/10.1016/j.msec.2016.11.073
7. U. Bulbake, S. Doppalapudi, N. Kommineni, W. Khan, Liposomal formulations in clinical use: an updated review, Pharmaceutics. 9 (2017) 12. https://doi.org/10.3390/pharmaceutics9020012.
8. A.K. Sharma, A. Gothwal, P. Kesharwani, H. Alsaab, A.K. Iyer, U. Gupta, Dendrimer nanoarchitectures for cancer diagnosis and anticancer drug delivery,Drug Discov Today. 22 (2017) 314-326.https://doi.org/10.1016/j.drudis.2016.09.013
9. Z. Li, A.L.B. de Barros, D.C.F. Soares, S.N. Moss, L. Alisaraie, Functionalized single-walled carbon nanotubes: cellular uptake, biodistribution and applications in drug delivery, Int. J. Pharm.524 (2017) 41-54.https://doi.org/10.1016/j.ijpharm.2017.03.017.
10. Y. Wang, Q. Zhao, N. Han, L. Bai, J. Li, J. Liu, E. Che, L. Hu, Q. Zhang, T. Jiang, Mesoporous silica nanoparticles in drug delivery and biomedical applications, Nanomed. Nanotechnol. Biol. Med.11 (2015) 313-327. https://doi.org/10.1016/j.nano.2014.09.014.
11. Y. Cao, N. Liu, C. Fu, K. Li, L. Tao, L. Feng, Y. Wei, Thermo and pH dual-responsive materials for controllable oil/water separation, ACS Appl. Mater. Interfaces. 6 (2014) 2026-2030. https://doi.org/ 10.1021/am405089m
12. K. Chen, J. Zhang, H. Gu, Dissolution from inside: a unique degradation behaviour of core–shell magnetic mesoporous silica nanoparticles and the effect of polyethyleneimine coating, J. Mater. Chem. 22 (2012) 22005-22012.
13. F. Martín-Saavedra, E. Ruíz-Hernández, A. Boré, D. Arcos, M. Vallet-Regí, N. Vilaboa, Magnetic mesoporous silica spheres for hyperthermia therapy, Acta Biomater. 6 (2010) 4522-4531. https://doi.org/10.1016/j.actbio.2010.06.030.
14. W.-H. Chen, G.-F. Luo, Q. Lei, F.-Y. Cao, J.-X. Fan, W.-X. Qiu, H.-Z. Jia, S. Hong, F. Fang, X. Zeng, Rational design of multifunctional magnetic mesoporous silica nanoparticle for tumor-targeted magnetic resonance imaging and precise therapy, Biomaterials.76 (2016) 87-101. https://doi.org/10.1016/j.biomaterials.2015.10.053.

15. P. Yang, S. Gai, J. Lin, Functionalized mesoporous silica materials for controlled drug delivery, Chem. Soc. Rev.41 (2012) 3679-3698.https://doi.org/ 10.1039/C2CS15308D.

16. M. Xuan, J. Shao, J. Zhao, Q. Li, L. Dai, J. Li, Cover Picture: Magnetic Mesoporous Silica Nanoparticles Cloaked by Red Blood Cell Membranes: Applications in Cancer Therapy ,Angew. Chem. Int. Ed. 57 (2018) 5955-5955. https://doi.org/10.1002/anie.201712996.
17. Z. Tian, X. Yu, Z. Ruan, M. Zhu, Y. Zhu, N. Hanagata, Magnetic mesoporous silica nanoparticles coated with thermo-responsive copolymer for potential chemo-and magnetic hyperthermia therapy, Microporous Mesoporous Mater. 256 (2018) 1-9. https://doi.org/10.1016/j.micromeso.2017.07.053.
18. A.H. Teruel, C. Coll, A.M. Costero, D. Ferri, M. Parra, P. Gaviña, M. González-Álvarez, V. Merino, M.D. Marcos, R. Martínez-Máñez, Functional Magnetic Mesoporous Silica Microparticles Capped with an Azo-Derivative: A Promising Colon Drug Delivery Device, Molecules, 23 (2018) 375.https://doi.org/ 10.3390/molecules23020375.
19. J. Kim, H.S. Kim, N. Lee, T. Kim, H. Kim, T. Yu, I.C. Song, W.K. Moon, T. Hyeon, Multifunctional uniform nanoparticles composed of a magnetite nanocrystal core and a mesoporous silica shell for magnetic resonance and fluorescence imaging and for drug delivery, Angew. Chem. Int. Ed. 120 (2008) 8566-8569. https://doi.org/10.1002/ange.200802469.
20. Q. Feng, Y. Liu, J. Huang, K. Chen, J. Huang, K. Xiao, Uptake, distribution, clearance, and toxicity of iron oxide nanoparticles with different sizes and coatings, Sci. Rep. 8 (2018) 2082.https://doi.org/10.1038/s41598-018-19628-z.
21. Y. Li, L. Sun, M. Jin, Z. Du, X. Liu, C. Guo, Y. Li, P. Huang, Z. Sun, Size-dependent cytotoxicity of amorphous silica nanoparticles in human hepatoma HepG2 cells, Toxicol. in Vitro. 25 (2011) 1343-1352. https://doi.org/10.1016/j.tiv.2011.05.003.

22. D. Napierska, L.C. Thomassen, V. Rabolli, D. Lison, L. Gonzalez, M. Kirsch-Volders, J.A. Martens, P.H. Hoet, Size-dependent cytotoxicity of monodisperse silica nanoparticles in human endothelial cells, Small. 5 (2009) 846-853. https://doi.org/10.1002/smll.200800461.
23. Y.-H. Lien, T.-M. Wu, Preparation and characterization of thermosensitive polymers grafted onto silica-coated iron oxide nanoparticles, J. Colloid Interface Sci.326 (2008) 517-521. https://doi.org/10.1016/j.jcis.2008.06.020.
24. F. Ye, S. Laurent, A. Fornara, L. Astolfi, J. Qin, A. Roch, A. Martini, M.S. Toprak, R.N. Muller, M. Muhammed, Uniform mesoporous silica coated iron oxide nanoparticles as a highly efficient, nontoxic MRI T2 contrast agent with tunable proton relaxivities, CONTRAST MEDIA MOL. 7 (2012) 460-468. https://doi.org/10.1002/cmmi.1473.
25. J. Liu, W. Bu, S. Zhang, F. Chen, H. Xing, L. Pan, L. Zhou, W. Peng, J. Shi, Controlled synthesis of uniform and monodisperse upconversion core/mesoporous silica shell nanocomposites for bimodal imaging, Chem. Eur. J.18 (2012) 2335-2341. https://doi.org/10.1002/chem.201102599.
26. H. Wen, J. Guo, B. Chang, W. Yang, pH-responsive composite microspheres based on magnetic mesoporous silica nanoparticle for drug delivery, Eur. J. Pharm. Biopharm. 84 (2013) 91-98. https://doi.org/10.1016/j.ejpb.2012.11.019.
27. J. Cichos, M. Karbowiak, A general and versatile procedure for coating of hydrophobic nanocrystals with a thin silica layer enabling facile biofunctionalization and dye incorporation, J. Mater. Chem. 2 (2014) 556-568. https://doi.org/ 10.1039/C3TB21442G.
28. C. Vogt, M.S. Toprak, M. Muhammed, S. Laurent, J.-L. Bridot, R.N. Müller, High quality and tuneable silica shell–magnetic core nanoparticles, J. Nanopart. Res.12 (2010) 1137-1147. https://doi.org/10.1007/s11051-009-9661-7.

29. C. Li, C. Ma, F. Wang, Z. Xi, Z. Wang, Y. Deng, N. He, Preparation and biomedical applications of core–shell silica/magnetic nanoparticle composites, J. Nanosci. Nanotechnol. 12 (2012) 2964-2972.
30. T. Kikuchi, R. Kasuya, S. Endo, A. Nakamura, T. Takai, N. Metzler-Nolte, K. Tohji, J. Balachandran, Preparation of magnetite aqueous dispersion for magnetic fluid hyperthermia, J Magn Magn Mater.323 (2011) 1216-1222. https://doi.org/10.1016/j.jmmm.2010.11.009.
31. A. Gutiérrez-Becerra, M. Barcena-Soto, V. Soto, J. Arellano-Ceja, N. Casillas, S. Prévost, L. Noirez, M. Gradzielski, J.I. Escalante, Structure of reverse microemulsion-templated metal hexacyanoferrate nanoparticles, Nanoscale Res. Lett.7 (2012) 83. https://doi.org/10.1186/1556-276X-7-83.
32. B. Chang, X. Sha, J. Guo, Y. Jiao, C. Wang, W. Yang, Thermo and pH dual responsive, polymer shell coated, magnetic mesoporous silica nanoparticles for controlled drug release, J. Mater. Chem. 21 (2011) 9239-9247.https://doi.org/10.1039/C1JM10631G.
33. S. Egodawatte, S. Dominguez Jr, S.C. Larsen, Solvent effects in the development of a drug delivery system for 5-fluorouracil using magnetic mesoporous silica nanoparticles, Microporous Mesoporous Mater. 237 (2017) 108-116.https://doi.org/10.1016/j.micromeso.2016.09.024.
34. D. Kala, J. Thomas, D.V. Nair, Effect of pH on aminofunctionalized mesoporous silica nanoparticles loaded with 5-fluorouracil and its optimization, Int J Pharm Pharm Sci. 7 (2018) 1400-1419.
35. H. Ding, Y. Zhang, S. Wang, J. Xu, S. Xu, G. Li, Fe3O4@ SiO2 core/shell nanoparticles: the silica coating regulations with a single core for different core sizes and shell thicknesses, Chem. Mater. 24 (2012) 4572-4580. https://doi.org/10.1016/10.1021/cm302828d.
36. J.A.R. Guivar, E.A. Sanches, C.J. Magon, E.G.R. Fernandes, Preparation and characterization of cetyltrimethylammonium bromide (CTAB)-stabilized Fe3O4 nanoparticles for electrochemistry detection of citric acid, J. Electroanal. Chem. 755 (2015) 158-166. https://doi.org/10.1016/j.jelechem.2015.07.036.
37. J.V. Hollingsworth, N.D.K. Bhupathiraju, J. Sun, E. Lochner, M.G.H. Vicente, P.S. Russo, Preparation of Metalloporphyrin-Bound Superparamagnetic Silica Particles via “Click” Reaction, ACS Appl. Mater. Interfaces. 8 (2016) 792-801.https://doi.org/ 10.1021/acsami.5b10034.
38. D.-S. Moon, J.-K. Lee, Formation of wrinkled silica mesostructures based on the phase behavior of pseudoternary systems, Langmuir. 30 (2014) 15574-15580.
39. C. Liu, J. Guo, W. Yang, J. Hu, C. Wang, S. Fu, Magnetic mesoporous silica microspheres with thermo-sensitive polymer shell for controlled drug release, J. Mater. Chem. 19 (2009) 4764-4770. https://doi.org/ 10.1039/B902985K.
40. Ab K. AbouAitah, A. Farghali, A. Swiderska-Sroda, W. Lojkowski, A. Razin, M. Khedr, pH-controlled release system for curcumin based on functionalized dendritic mesoporous silica nanoparticles, J Nanomed Nanotechnol. 7 (2016) 1. http://dx.doi.org/10.4172/2157-7439.1000351.

Highlights

Inverse microemulsion system was used to synthesize iron oxide/mesoporous silica nanoparticles with core/shell structure.

Urea was used as a weak base catalyst to control the aggregation of the nanoparticles.

Nanocomposites were less than 100 nm in diameter.

The factors that control silica thickness were identified.